Biochemical and Biophysical Research Communications 625 (2022) 116–121

Contents lists available at ScienceDirect

Biochemical and Biophysical Research Communications

journal homepage: www.elsevier.com/locate/ybbrc

Effects of a selective PPARα modulator, sodium-glucose cotransporter 2 inhibitor, and statin on the myocardial morphology of medaka nonalcoholic fatty liver disease model

Marina Ohkoshi-Yamada [a], Kenya Kamimura [a, b, *], Atsushi Kimura [a], Yuto Tanaka [a], Itsuo Nagayama [a], Shunta Yakubo [a], Hiroyuki Abe [a], Takeshi Yokoo [a], Akira Sakamaki [a], Hiroteru Kamimura [a], Shuji Terai [a]

[a] Division of Gastroenterology and Hepatology, Graduate School of Medical and Dental Sciences, Niigata University, 1-757, Asahimachi-Dori, Chuo-Ku, Niigata, Japan
[b] Department of General Medicine, Niigata University School of Medicine, 1-757, Asahimachi-Dori, Chuo-Ku, Niigata, Japan

ARTICLE INFO

Article history:
Received 24 July 2022
Received in revised form
27 July 2022
Accepted 31 July 2022
Available online 3 August 2022

Keywords:
Nonalcoholic fatty liver disease
Heart disease
Medaka
Selective peroxisome proliferator-activated receptor alpha
Sodium-glucose cotransporter 2 inhibitor
Statin

ABSTRACT

Objective: Nonalcoholic fatty liver disease (NAFLD) is associated with metabolic dysregulation and is linked with various cardiovascular complications, which often lead to poor prognostic outcomes. To develop a standard therapy for NAFLD and to urgently address its complications, the current study aimed to investigate the mechanisms of NAFLD-related heart disease and the therapeutic effects of drugs targeting various metabolic pathways.

Methods: To explore the mechanism of NAFLD-related heart disease, a medaka model of high-fat diet-induced NAFLD was utilized. The gross structural, histological, and inflammatory changes in the myocardium were evaluated in a time-dependent manner. In addition, the therapeutic effects of medicines used for NAFLD treatment including, selective peroxisome proliferator-activated receptor α modulator (SPPARMα, pemafibrate), sodium-glucose cotransporter 2 (SGLT2) inhibitor (tofogliflozin), and statin (pitavastatin), and their combinations on heart pathology were evaluated. To determine the mechanisms underlying the therapeutic effects, the expression of genes related to liver inflammation was assessed via whole transcriptome sequencing analysis.

Results: The fish with NAFLD-related heart injury presented with cardiomyocyte hypertrophy, which led to cardiac hypertrophy. This morphological change was caused by the infiltration of inflammatory cells, including macrophages and $CD4^{-}$ and CD8-positive lymphocytes, in the cardiac wall and the expression of transforming growth factor beta 1 in the cardiomyocytes.

Further, the livers of the fish had upregulated expressions of senescence-associated secretory phenotype-related genes. Treatment with pemafibrate, tofogliflozin, and pitavastatin reduced these changes and, consequently, cardiomyopathy.

Conclusion: Our results demonstrated that NAFLD-related heart disease was attributed to the senescence-associated secretory phenotype-induced inflammatory activity in the cardiac wall, which resulted in myocardial hypertrophy. Moreover, the effects of SPPARMα, SGLT2 inhibitor, and statin on NAFLD-related heart disease were evident in the medaka NAFLD model.

1. Introduction

The incidence of nonalcoholic fatty liver disease (NAFLD) is increasing, and NAFLD is commonly associated with complications in various organ systems, including the liver, kidneys, and heart [1,2]. In patients with NAFLD, cardiovascular system complications, such as coronary heart diseases and hypertrophic cardiomyopathy, are the most frequent causes of mortality, followed by extra-hepatic cancers and liver-related conditions [3]. These complications may cause sudden death, arrhythmia, and heart failure, which are significantly correlated with poor prognosis [3–6]. Therefore, the mechanisms of NAFLD-related heart disease should be explored, and effective therapeutic options must be developed. Based on

* Corresponding author. Division of Gastroenterology and Hepatology, Graduate School of Medical and Dental Sciences, Niigata University, Japan.
E-mail address: kenya-k@med.niigata-u.ac.jp (K. Kamimura).

https://doi.org/10.1016/j.bbrc.2022.07.117
0006-291X/

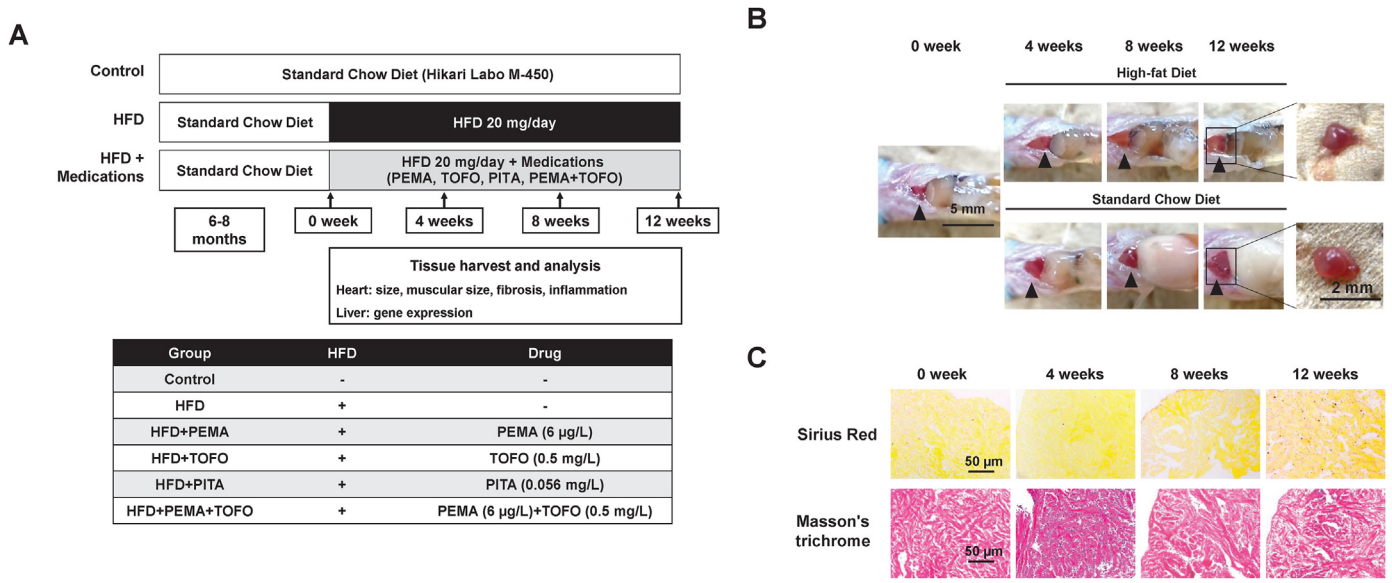

Group	HFD	Drug
Control	-	-
HFD	+	-
HFD+PEMA	+	PEMA (6 μg/L)
HFD+TOFO	+	TOFO (0.5 mg/L)
HFD+PITA	+	PITA (0.056 mg/L)
HFD+PEMA+TOFO	+	PEMA (6 μg/L)+TOFO (0.5 mg/L)

Fig. 1. Study design and development of the HFD-induced heart disease medaka model
(A) Schematic presentation of the study design. HFD, high-fat diet; PEMA, pemafibrate; TOFO, tofogliflozin; PITA, pitavastatin. **(B)** Time-dependent changes in the heart of HFD-fed medaka. **(C)** Representative images of Sirius Red and Masson's trichrome staining of the heart. The scale bar represents 50 μm. (For interpretation of the references to colour in this figure legend, the reader is referred to the Web version of this article.)

these points of view, therapeutic options targeting metabolic dysregulation, which causes these complications, could be effective [2]. Recent reports have shown that selective peroxisome proliferator-activated receptor alpha modulator (SPPARMα) (pemafibrate, PEMA) [7–10], sodium–glucose cotransporter 2 inhibitor (SGLT2i) [11–14], and statin [15,16] are effective in decreasing cardiovascular events in patients with NAFLD. However, the minute mechanisms underlying the pathogenesis of NAFLD-related heart disease and the therapeutic effects of drugs have not been identified. Based on previous studies, a medaka disease model reproduced the pathogenesis of human diseases including NAFLD via HFD feeding. Thus, it can be an appropriate animal model for examining the mechanisms and therapeutic effects of various medications [17–20]. Therefore, we have examined the pathogenesis of NAFLD-related heart disease and evaluated the therapeutic effect of SPPARMα, SGLT2i, and statin using a medaka NAFLD model in this study.

2. Materials and methods

2.1. Animals

All animals received humane care according to the criteria outlined in the Guide for the Care and Use of Laboratory Animals by the National Academy of Sciences (the USA). The study protocol was approved (nos. 00424, 00804, and 01078), and the experiments were conducted based on the regulations of the Institutional Animal Care and Use Committee of Niigata University (Niigata, Japan). The d-rR/Tokyo strain medaka fish (strain ID: MT837) was supplied by NBRP Medaka (https://shigen.nig.ac.jp/medaka/). Male fish aged 6 months were used in the experiment and maintained in plastic tanks (Nacalai Tesque, Kyoto, Japan) containing 2 L of tap water with temperature maintained at 25 °C ± 1 °C, under fluorescent light from 8 a.m. to 8 p.m.

2.2. Development of the medaka NAFLD model

The medaka NAFLD model was developed via high-fat diet (HFD) feeding (HFD32; CLEA Japan, Tokyo, Japan) using a method reported in previous studies [18–20]. Briefly, each tank was supplied with a control diet (Hikari Labo M-450; Kyorin, Hyogo, Japan) or HFD at 20 mg/fish daily, and all food provided were consumed within 14 h. The energy content of the control standard diet was 3.8 kcal/g, with 23.2% of calories derived from fat, 44.0% from protein, and 32.7% from carbohydrate; vitamins and minerals were provided as recommended (Hikari Labo M-450; Kyorin Co. Ltd, Hyogo, Japan). In total, 6–7 (>30) medakas each from the HFD, HFD + PEMA, HFD + tofogliflozin (TOFO), HFD + pitavastatin (PITA), and HFD + PEMA + TOFO groups were prepared and analyzed at each time point. Each experiment was repeated three times to confirm the results. Therefore, approximately 360 medakas were evaluated.

2.3. Drug administration

PEMA, TOFO, and PITA (Kowa Co., Ltd., Tokyo, Japan) were dissolved in dimethyl sulfoxide to maintain the drug concentrations in the water tanks. The final concentration of these drugs was determined using methods in our previous studies [18–20]. The same volume of dimethyl sulfoxide was administered to the tank of the HFD group. The water, HFD, and drug in the tank were replaced every 2 days, and the tanks were cautiously washed to maintain a consistent concentration.

2.4. Histological analyses

Tissue samples were collected from the myocardium at appropriate time points, fixed in 10% formalin, and embedded in paraffin. Then, 10-μm-thick sections were stained with hematoxylin and eosin, Sirius Red, or Masson's trichrome. The heart size was measured at its vertical axis, and the cardiomyocyte diameter was evaluated at the level of the nucleus in the longitudinal sections of the interventricular septum [21].

The following agents were used in immunohistochemical staining: anti-transforming growth factor beta 1 (TGF-β1) antibody (sc-130348, Santa Cruz Biotechnology, Dallas, TX, the USA) at 1:200 dilution with VECTASTAIN Elite ABC Mouse IgG Kit (PK-6102, Vector

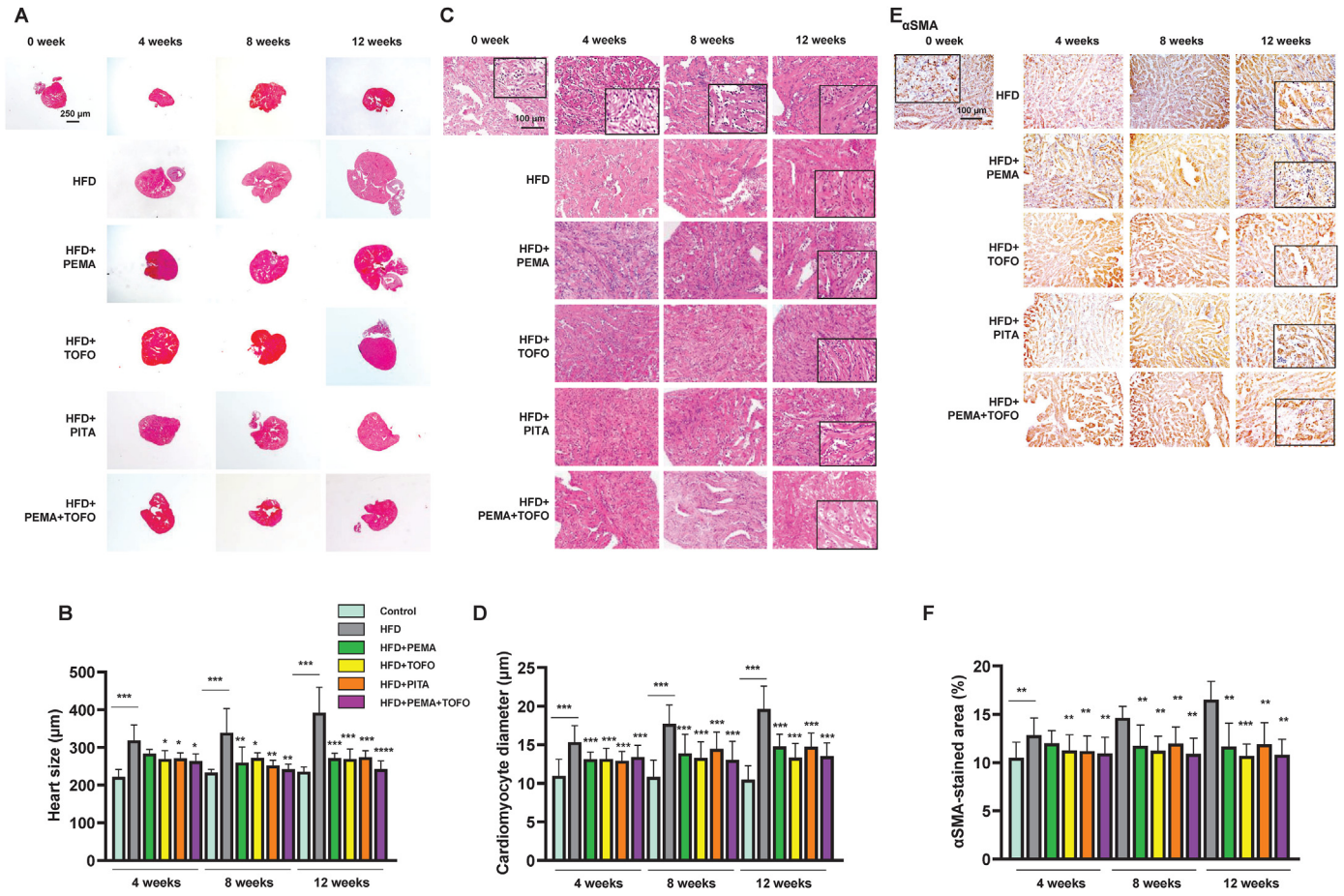

Fig. 2. Structural changes in the heart of NAFLD medaka and the effect of medications
(A) Time-dependent changes in the heart size of each group. Representative microscopic findings of medaka heart (hematoxylin and eosin staining). The scale bar represents 250 μm. **(B)** Quantitative analysis of the heart size. The values represent mean ± SD (n = 15 for each group). $*p < 0.05$, $**p < 0.01$, and $***p < 0.001$ compared with the HFD group at each time point. Student's *t*-test. **(C)** Time-dependent changes in the diameter of cardiomyocytes in each group. Representative images of medaka cardiomyocytes stained with hematoxylin and eosin. **(D)** Quantitative analysis of the cardiomyocyte diameter. The scale bar represents 100 μm. The images in the insets show the larger images. The values represent mean ± SD (n = 15 for each group). $***p < 0.001$ compared with the HFD group at each time point. Student's *t*-test. **(E)** Representative microscopic findings of the cardiomyocytes of HFD-fed medaka (αSMA staining). **(F)** Quantitative analysis of the area that stained positive for αSMA. The scale bar represents 100 μm. The images in the insets show the larger images. The values represent mean ± SD (n = 15 for each group). $**p < 0.01$ and $***p < 0.001$ compared with the HFD group at each time point. Student's *t*-test. NAFLD, nonalcoholic fatty liver disease; HFD, high-fat diet; PEMA, pemafibrate, TOFO, tofogliflozin, PITA, pitavastatin.

Laboratories, Burlingame, CA, USA) and 3,3′-Diaminobenzidine (DAB) chromogen tablets (Muto Pure Chemicals, Tokyo, Japan); anti-alpha smooth muscle actin (αSMA) antibody (ab5694, Abcam, MA, USA) at 1:200 dilution; anti-F4/80 antibody (ab111101, Abcam) at 1:100 dilution; anti-CD4 antibody (ab183685, Abcam) at 1:1000 dilution; and anti-CD8 alpha antibody (ab101500, Abcam) at 1:50 dilution with VECTASTAIN Elite ABC Rabbit IgG Kit (PK-6101, Vector Laboratories) and DAB chromogen tablets (Muto Pure Chemicals, Tokyo, Japan). Then, the images of each tissue section were captured randomly, and quantitative analysis was performed with ImageJ (version 1.8.0_172, National Institutes of Health, USA) with the RGB-based protocol, as reported in previous studies [22].

2.5. Whole transcriptome sequencing

Whole transcriptome sequencing of *Oryzias latipes* (Japanese medaka) was performed to investigate the gene expression profiles in the liver of NAFLD medaka with/without PEMA, TOFO, and PITA treatment (Macrogen Japan Corp., Koto City, Tokyo, Japan), as reported in a previous study [20]. During data preprocessing, low-quality transcripts were filtered; hence, from a total of 27,067 genes, 4046 genes were used in the statistical analysis of samples. In groups with different conditions, differentially expressed genes or transcripts were confirmed by testing the statistical hypothesis. Then, the expressions of genes related to the inflammation were compared among the groups, and gene expressions with more than two-fold differences were presented in the heat map.

2.6. Statistical analyses

Data from each group are presented as the mean ± standard deviation. Differences were evaluated using either one-way analysis of variance (ANOVA), followed by the Tukey's multiple comparison test, or the Student's t-test using GraphPad Prism 9 software (version 9.3.1; GraphPad, San Diego, CA, USA). A p value of <0.05 was considered to indicate statistical significance.

3. Results

3.1. Effects of HFD on the cardiac structure of medaka

To investigate the effects of HFD on the cardiac structure, the medaka NAFLD model was developed via HFD feeding, as reported in previous studies [18–20] (Fig. 1A). Fig. 1B shows the time-

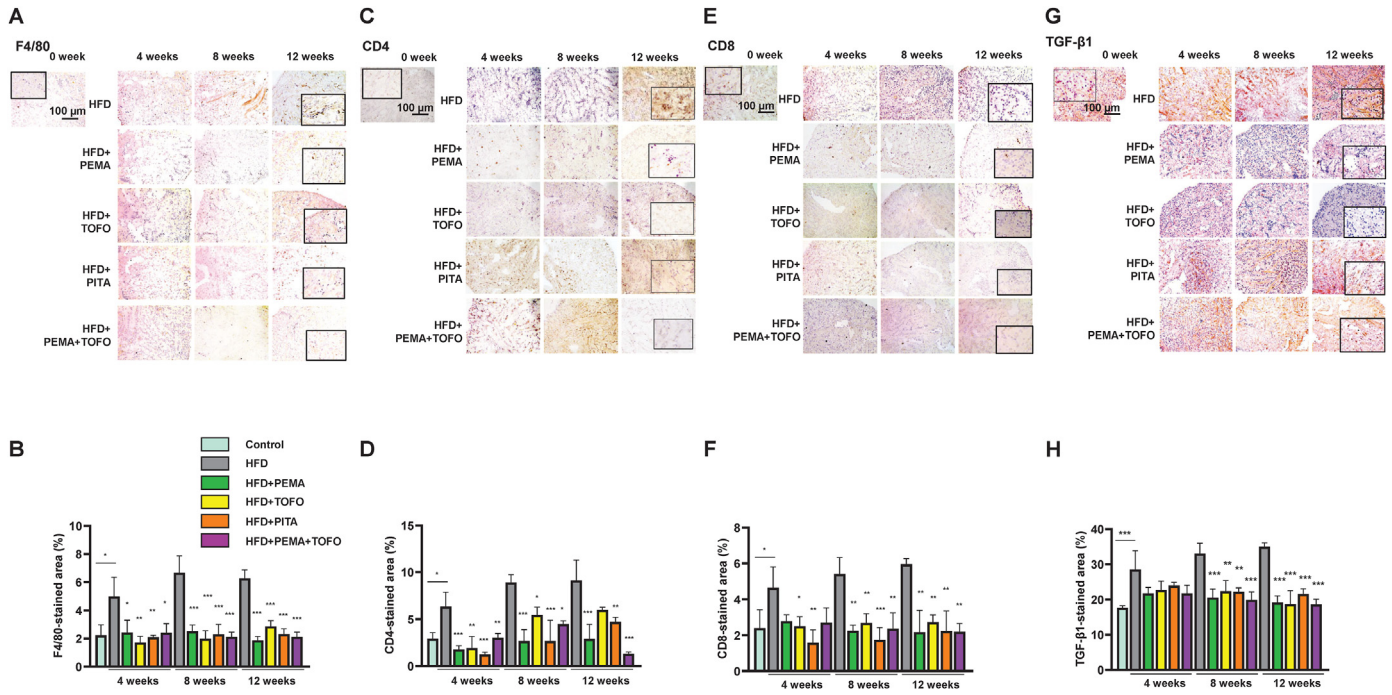

Fig. 3. Infiltration of inflammatory cells in the heart of HFD-fed medaka
(A) Representative microscopic findings of the cardiomyocytes of HFD-fed medaka (F4/80 staining). **(B)** Quantitative analysis of the F4/80-positive area. The scale bar represents 100 μm. The images in the insets show the larger images. The values represent mean ± SD (n = 15 for each group). *$p < 0.05$, **$p < 0.01$, and ***$p < 0.001$ compared with HFD group at each time point. Student's *t*-test. **(C)** Representative microscopic findings of the cardiomyocytes of HFD-fed medaka (CD4 staining). **(D)** Quantitative analysis of the CD4-positive area. The scale bar represents 100 μm. Images in the insets show the larger images. The values represent mean ± SD (n = 15 for each group). *$p < 0.05$, **$p < 0.01$, and ***$p < 0.001$ compared with the HFD group at each time point. Student's *t*-test. **(E)** Representative microscopic findings of the cardiomyocytes of HFD-fed medaka (CD8 staining). **(F)** Quantitative analysis of CD8-positive area. The scale bar represents 100 μm. Images in the insets show the larger images. The values represent mean ± SD (n = 15 for each group). *$p < 0.05$ and **$p < 0.01$ compared with the HFD group at each time point. Student's *t*-test. **(G)** Representative microscopic findings of the cardiomyocytes of HFD-fed medaka (TGF-β1 staining). **(H)** Quantitative analysis of the TGF-β1 positive area. The scale bar represents 100 μm. Images in the insets show the larger images. The values represent mean ± SD (n = 15 for each group). **$p < 0.01$ and ***$p < 0.001$ compared with the HFD group at each time point. Student's *t*-test. PEMA, pemafibrate, TOFO, tofogliflozin, PITA, pitavastatin.

dependent macroscopic changes in the hearts of HFD-fed medaka. Sirius Red and Masson's trichrome staining showed no significant fibrotic tissues in the heart (Fig. 1C). Then, the heart size of HFD-fed medaka was assessed using hematoxylin and eosin staining images at a low magnification (Fig. 2A). HFD-fed medaka had a significantly larger heart size than control chow-fed medaka and showed its increase in a time-dependent manner. This size change was alleviated with treatment by PEMA, TOFO, PITA, and PEMA + TOFO administration (Fig. 2A and B). Based on the microscopic findings of hematoxylin and eosin and αSMA staining, the diameter of the cardiomyocytes increased with HFD feeding and reduced with the medications (Fig. 2C–F). Compared with other medications, combination of PEMA and TOFO (PEMA + TOFO) was more effective in preventing heart and cardiomyocyte size increase. These results suggest that the medaka fish with NAFLD-related heart disease mainly presented with enlarged cardiomyocytes, which cause hypertrophic cardiac changes.

3.2. Effect of inflammation in the heart of HFD-fed medaka

As the inflammatory cell infiltration [23] and TGF-β1 induce hypertrophy of the cardiomyocyte [24,25], the effects of inflammatory cell infiltration and TGF-β1 on the pathologies of NAFLD-related heart disease were evaluated using the medaka model. HFD-fed medaka had a significantly higher number of F4/80-, CD4-, and CD8-positively stained cells than chow-fed medaka. Moreover, the number of stained cells increased in a time-dependent manner (Fig. 3A–F). TGF-β1 staining showed that the size of the positively stained area in the cardiomyocyte of medaka increased with HFD feeding (Fig. 3G and H) and decreased with treatment by PEMA, TOFO, PITA, and PEMA + TOFO administration, while the drugs' effects did not significantly differ (Fig. 3). These results suggest that the inflammatory cell infiltration and TGF-β1 activation induced cardiomyocyte hypertrophy within 12 weeks. In addition, NAFLD treatment resulted in milder changes in the heart.

3.3. Effect of changes in inflammation-related gene expressions on the heart of HFD-fed medaka

NAFLD treatment reduced inflammation in the heart; however, its associated mechanism has not been elucidated. Therefore, whole transcriptome sequencing of hepatocytes was performed to examine changes in the expression of various genes in the medaka NAFLD model (Fig. 4). Results showed that the expression of genes including; nuclear factor kappa B subunit 2, forkhead box O4, elongation factor 1 alpha, cyclin-dependent kinase inhibitor 1C, mechanistic target of rapamycin kinase, glycogen phosphorylase L, notch receptor 1, immunoglobulin-like domain containing receptor 2, etc. showed significant difference between HFD-fed medaka and control, PEMA, TOFO, PITA, or PEMA + TOFO treated groups (Fig. 4).

4. Discussion

NAFLD causes various organ damages, including cardiovascular complications [3,26–28], and it is the leading cause of mortality among patients with NAFLD [3]. Heart injury in humans is caused by systemic inflammation and cardiomyocyte insulin resistance, which lead to muscular damage and pressure and volume overload

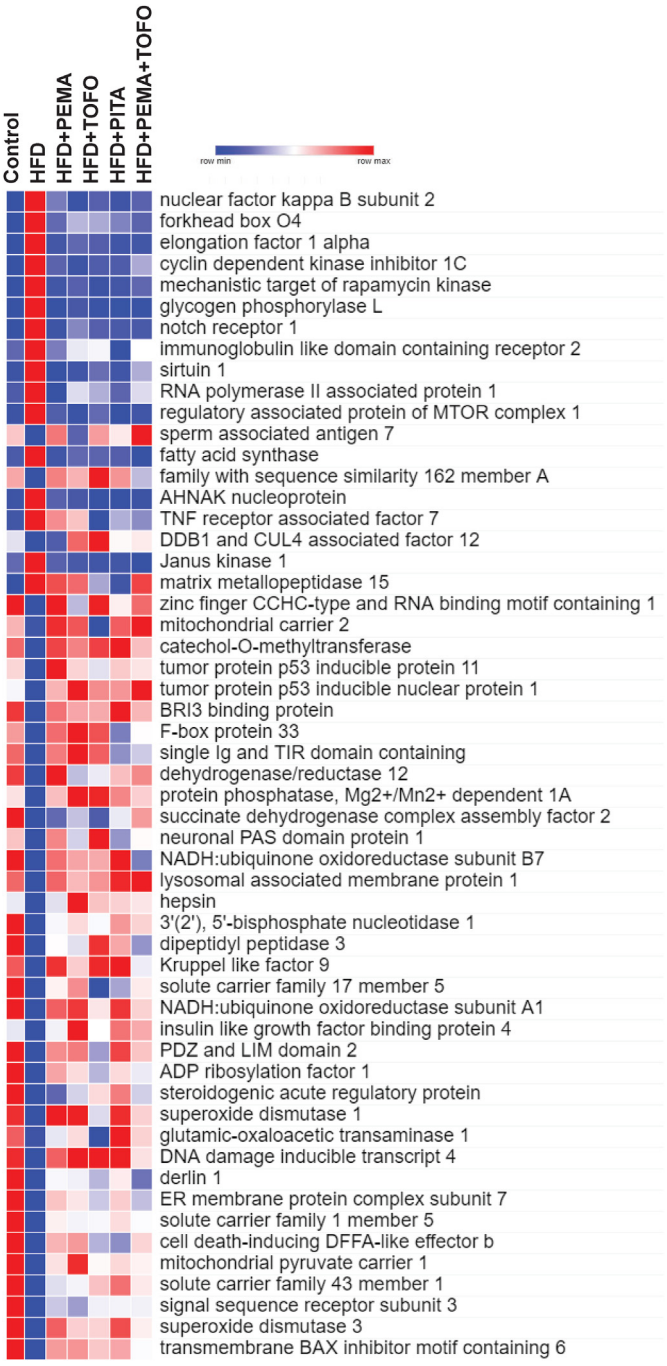

Fig. 4. Heatmap for differentially expressed, inflammation-related genes in the livers of medaka

The expressions of genes related to the inflammation were compared among the groups and gene expressions with more than two-fold differences were shown in the heat map. PEMA, pemafibrate, TOFO, tofogliflozin, PITA, pitavastatin.

in the heart and induces cardiovascular events such as arrhythmia and heart failure [3–6]. Therefore, an understanding of its pathogenesis and management are essential in improving the prognosis of patients with NAFLD. Our study demonstrated that the medaka NAFLD model reproduced the infiltration of inflammatory cells, including macrophages and CD4- and CD8-positive lymphocytes, in the cardiac wall and the expression of TGF-β1 in the cardiomyocytes caused hypertrophic morphological changes in the heart. In addition, systemic inflammation is partly correlated with the activated expressions of senescence-associated secretory phenotype (SASP)-related genes in the hepatocytes in NAFLD. To date, a clinical study further showed the potential contribution of cytokines [5,6] and TGF-β1 on muscular hypertrophy and fibrotic changes [24,25], and *in vivo* animal studies revealed infiltration of inflammatory cells in the heart of NAFLD mice [23,24]. However, the origin of the inflammation in this pathology has not been elucidated. As previous studies have shown that the senescence and elimination of HFD-damaged hepatocytes lead to the recovery of NAFLD [29,30]; it is reasonable that, in HFD-fed NAFLD medaka animal model, SASP from the liver induces inflammatory cell infiltration in other organs, which leads to NAFLD-related multi-organ pathogenesis.

Our results showed that treatment with PEMA, TOFO, and PITA suppressed the expression of SASP-related genes in the hepatocytes and inflammatory cell infiltration in the heart, thereby consequently alleviating HFD-induced heart injury in medaka. This finding is consistent with clinical data showing that PEMA [7–9], SGLT2i [11–14], and statin [15,16] are effective in reducing cardiovascular events in NAFLD. Thus, our results supported the notion that therapeutic options targeting metabolic pathways could achieve better control of NAFLD-related organ damage [2]. The current study had several limitations. That is, molecular-based analysis of the association between NAFLD pathogenesis and senescence and pharmacological assessment of the senolytic effect of medications tested were not performed. Nevertheless, further studies assessing the direct effect of senomorphic drug on NAFLD-related heart disease in the models should be performed. In addition, as NAFLD-related heart damage eventually causes fibrotic changes [5,6,24,25], studies with a longer duration should be conducted to examine advanced morphological changes and the therapeutic efficacy of medications.

In conclusion, this study showed for the first time that the SASP of HFD-damaged hepatocytes resulted in NAFLD-related heart injury by inducing the inflammatory changes in the heart. In addition, SPPARMα, statin, and SGLT2i reduced the SASP activation and inflammatory changes in the cardiac wall and hypertrophic morphological change of the heart, hence these medicines can be the candidate for the therapeutic options for NAFLD-related heart disease.

Funding

The research was supported in part by Grant-in-Aid for Scientific Research from the Japanese Society for the Promotion of Sciences 25670370, 16K15424, and 21K19478 to Terai S and Kamimura K. This work was partly supported by Kowa Co., Ltd. The funders had no role in the study design, data collection and analysis, and manuscript preparation and publication.

Author contributions

MO-Y, KK, AK, and ST contributed to the study conception and design. Material preparation, data collection, and analysis were performed by MO-Y, KK, AK, YT, IN, SY, HA, TY, AK, HK, and ST. The first draft of the manuscript was written by MO-Y, KK, and ST, and all authors read and approved the final manuscript.

Declaration of competing interest

The authors declare that they have no competing interests.

Acknowledgments

The authors would like to thank Takao Tsuchida in the Division of Gastroenterology and Hepatology at the Niigata University for his

excellent assistance in the histological analyses. The authors would also like to thank Nobuyoshi Fujisawa, Kanako Oda, Shuko Adachi, Katsuya Hirasawa, Takenori Sakuma, Toshikuni Sasaoka, and all staff members at the Division of Laboratory Animal Resources in Niigata University.

References

[1] M. El-Kassas, J. Cabezas, P. Iruzubieta, M.H. Zheng, J.P. Arab, A. Awad, Non-alcoholic fatty liver disease: current global burden, Semin. Liver Dis. (2022), https://doi.org/10.1055/a-1862-9088. In press.
[2] R. Loomba, S.L. Friedman, G.I. Shulman, Mechanisms and disease consequences of nonalcoholic fatty liver disease, Cell 184 (2021) 2537–2564.
[3] A. Mantovani, E. Scorletti, A. Mosca, A. Alisi, C.D. Byrne, G. Targher, Complications, morbidity and mortality of nonalcoholic fatty liver disease, Metabolism 111S (2020) 154170, https://doi.org/10.1016/j.metabol.2020.154170.
[4] G. Targher, L. Bertolini, F. Poli, S. Rodella, L. Scala, R. Tessari, L. Zenari, G. Falezza, Nonalcoholic fatty liver disease and risk of future cardiovascular events among type 2 diabetic patients, Diabetes 54 (2005) 3541–3546, https://doi.org/10.2337/diabetes.54.12.3541.
[5] A. Mantovani, S. Ballestri, A. Lonardo, G. Targher, Cardiovascular disease and myocardial abnormalities in nonalcoholic fatty liver disease, Dig. Dis. Sci. 61 (2016) 1246–1267, https://doi.org/10.1007/s10620-016-4040-6.
[6] T.G. Simon, D.G. Bamira, R.T. Chung, R.B. Weiner, K.E. Corey, Nonalcoholic steatohepatitis is associated with cardiac remodeling and dysfunction, Obesity 25 (2017) 1313–1316, https://doi.org/10.1002/oby.21879. Erratum in: Obesity (Silver Spring), 25 (2017) 1639–1640.
[7] H. Kawanishi, K. Ohashi, H. Ogawa, N. Otaka, T. Takikawa, L. Fang, Y. Ozaki, M. Takefuji, T. Murohara, N. Ouchi, A novel selective PPARα modulator, pemafibrate promotes ischemia-induced revascularization through the eNOS-dependent mechanisms, PLoS One 15 (2020), e0235362.
[8] Y. Honda, T. Kessoku, Y. Ogawa, W. Tomeno, K. Imajo, K. Fujita, M. Yoneda, T. Takizawa, S. Saito, Y. Nagashima, A. Nakajima, Pemafibrate, a novel selective peroxisome proliferator-activated receptor alpha modulator, improves the pathogenesis in a rodent model of nonalcoholic steatohepatitis, Sci. Rep. 7 (2017) 42477.
[9] A. Nakajima, Y. Eguchi, M. Yoneda, K. Imajo, N. Tamaki, H. Suganami, T. Nojima, R. Tanigawa, M. Iizuka, Y. Iida, R. Loomba, Randomised clinical trial: pemafibrate, a novel selective peroxisome proliferator-activated receptor α modulator (SPPARMα), versus placebo in patients with non-alcoholic fatty liver disease, Aliment. Pharmacol. Ther. 54 (2021) 1263–1277.
[10] S. Guixé-Muntet, L. Biquard, G. Szabo, J.F. Dufour, F. Tacke, S. Francque, P.E. Rautou, J. Gracia-Sancho, Review article: vascular effects of PPARs in the context of NASH, Aliment. Pharmacol. Ther. 56 (2022) 209–223, https://doi.org/10.1111/apt.17046.
[11] Q.Q. Zhang, G.Q. Li, Y. Zhong, J. Wang, A.N. Wang, X. Zhou, X.M. Mao, Empagliflozin improves chronic hypercortisolism-induced abnormal myocardial structure and cardiac function in mice, Ther. Adv. Chronic Dis. 11 (2020), https://doi.org/10.1177/2040622320974833, 2040622320974833.
[12] B. Neal, V. Perkovic, K.W. Mahaffey, D. de Zeeuw, G. Fulcher, N. Erondu, W. Shaw, G. Law, M. Desai, D.R. Matthews, CANVAS program collaborative group, canagliflozin and cardiovascular and renal events in type 2 diabetes, N. Engl. J. Med. 377 (2017) 644–657.
[13] M. Yoneda, Y. Honda, Y. Ogawa, T. Kessoku, T. Kobayashi, K. Imajo, A. Ozaki, A. Nogami, M. Taguri, T. Yamanaka, H. Kirikoshi, T. Iwasaki, T. Kurihashi, S. Saito, A. Nakajima, Comparing the effects of tofogliflozin and pioglitazone in non-alcoholic fatty liver disease patients with type 2 diabetes mellitus (ToP-iND study): a randomized prospective open-label controlled trial, BMJ Open Diabetes Res. Care. 9 (2021), e001990.
[14] C. Wanner, N. Marx, SGLT2 inhibitors: the future for treatment of type 2 diabetes mellitus and other chronic diseases, Diabetologia 61 (2018) 2134–2139, https://doi.org/10.1007/s00125-018-4678-z.
[15] M.J. Thomson, M. Serper, V. Khungar, L.M. Weiss, H. Trinh, R. Firpi-Morell, M. Roden, R. Loomba, A.S. Barritt 4th, D. Gazis, A.R. Mospan, M.W. Fried, K.R. Reddy, A.S. Lok, Prevalence and factors associated with statin use Among patients with nonalcoholic fatty liver disease in the TARGET-NASH study, Clin. Gastroenterol. Hepatol. 20 (2022) 458–460, https://doi.org/10.1016/j.cgh.2021.03.031, e4.
[16] H. Hyogo, T. Ikegami, K. Tokushige, E. Hashimoto, K. Inui, Y. Matsuzaki, H. Tokumo, F. Hino, S. Tazuma, Efficacy of pitavastatin for the treatment of non-alcoholic steatohepatitis with dyslipidemia: an open-label, pilot study, Hepatol. Res. 41 (2011) 1057–1065.
[17] Y. Shinagawa-Kobayashi, K. Kamimura, R. Goto, K. Ogawa, R. Inoue, T. Yokoo, N. Sakai, T. Nagoya, A. Sakamaki, S. Abe, S. Sugitani, M. Yanagi, K. Fujisawa, Y. Nozawa, N. Koyama, H. Nishina, M. Furutani-Seiki, I. Sakaida, S. Terai, Effect of histidine on sorafenib-induced vascular damage: analysis using novel medaka fish model, Biochem. Biophys. Res. Commun. 496 (2018) 556–561.
[18] R. Goto, K. Kamimura, Y. Shinagawa-Kobayashi, N. Sakai, T. Nagoya, Y. Niwa, M. Ko, K. Ogawa, R. Inoue, T. Yokoo, A. Sakamaki, H. Kamimura, S. Abe, H. Nishina, S. Terai, Inhibition of sodium glucose cotransporter 2 (SGLT2) delays liver fibrosis in a medaka model of nonalcoholic steatohepatitis (NASH), FEBS Open Bio 9 (2019) 643–652.
[19] T. Nagoya, K. Kamimura, R. Goto, Y. Shinagawa-Kobayashi, Y. Niwa, A. Kimura, N. Sakai, M. Ko, H. Nishina, S. Terai, Inhibition of sodium-glucose cotransporter 2 ameliorates renal injury in a novel medaka model of nonalcoholic steatohepatitis-related kidney disease, FEBS Open Bio 9 (2019) 2016–2024.
[20] A. Kimura, K. Kamimura, M. Ohkoshi-Yamada, Y. Shinagawa-Kobayashi, R. Goto, T. Owaki, C. Oda, O. Shibata, S. Morita, N. Sakai, H. Abe, T. Yokoo, A. Sakamaki, H. Kamimura, S. Terai, Effects of a novel selective PPARα modulator, statin, sodium-glucose cotransporter 2 inhibitor, and combinatorial therapy on the liver and vasculature of medaka nonalcoholic steatohepatitis model, Biochem. Biophys. Res. Commun. 596 (2022) 76–82, https://doi.org/10.1016/j.bbrc.2022.01.086.
[21] D. Baudouy, J.F. Michiels, A. Vukolic, K.D. Wagner, N. Wagner, Echocardiographic and histological examination of cardiac morphology in the mouse, J. Vis. Exp. 128 (2017) 55843, https://doi.org/10.3791/55843.
[22] T. Vrekoussis, V. Chaniotis, I. Navrozoglou, V. Dousias, K. Pavlakis, E.N. Stathopoulos, O. Zoras, Image analysis of breast cancer immunohistochemistry-stained sections using ImageJ: an RGB-based model, Anticancer Res. 29 (2009) 4995–4998.
[23] H. Kondo, I. Abe, K. Gotoh, A. Fukui, H. Takanari, Y. Ishii, Y. Ikebe, S. Kira, T. Oniki, S. Saito, K. Aoki, T. Tanino, K. Mitarai, K. Kawano, M. Miyoshi, M. Fujinami, S. Yoshimura, R. Ayabe, N. Okada, Y. Nagano, H. Akioka, T. Shinohara, K. Akiyoshi, T. Masaki, Y. Teshima, K. Yufu, M. Nakagawa, N. Takahashi, Interleukin 10 treatment ameliorates high-fat diet-induced inflammatory atrial remodeling and fibrillation, Circ. Arrhythm. Electrophysiol. 11 (2018), e006040. HTTPS://doi.org/10.1161/CIRCEP.117.006040.
[24] V. Rai, P. Sharma, S. Agrawal, D.K. Agrawal, Relevance of mouse models of cardiac fibrosis and hypertrophy in cardiac research, Mol. Cell. Biochem. 424 (2017) 123–145, https://doi.org/10.1007/s11010-016-2849-0.
[25] Q. Li, X. Liu, J. Wei, Ageing related periostin expression increase from cardiac fibroblasts promotes cardiomyocytes senescent, Biochem. Biophys. Res. Commun. 452 (2014) 497–502, https://doi.org/10.1016/j.bbrc.2014.08.109 (Epub 2014 Aug 27). PubMed: 25173938.
[26] C.D. Byrne, G. Targher, NAFLD as a driver of chronic kidney disease, J. Hepatol. 72 (2020) 785–801, https://doi.org/10.1016/j.jhep.2020.01.013.
[27] M.J. Armstrong, L.A. Adams, A. Canbay, W.K. Syn, Extrahepatic complications of nonalcoholic fatty liver disease, Hepatology 59 (2014) 1174–1197, https://doi.org/10.1002/hep.26717.
[28] Q.M. Anstee, A. Mantovani, H. Tilg, G. Targher, Risk of cardiomyopathy and cardiac arrhythmias in patients with nonalcoholic fatty liver disease, Nat. Rev. Gastroenterol. Hepatol. 15 (2018) 425–439, https://doi.org/10.1038/s41575-018-0010-0.
[29] J.H. Wang, L. Zhao, X. Pan, N.N. Chen, J. Chen, Q.L. Gong, F. Su, J. Yan, Y. Zhang, S.H. Zhang, Hypoxia-stimulated cardiac fibroblast production of IL-6 promotes myocardial fibrosis via the TGF-β1 signaling pathway, Lab. Invest. 96 (2016) 839–852, https://doi.org/10.1038/labinvest.2016.65.
[30] S. Omori, T.W. Wang, Y. Johmura, T. Kanai, Y. Nakano, T. Kido, E.A. Susaki, T. Nakajima, S. Shichino, S. Ueha, M. Ozawa, K. Yokote, S. Kumamoto, A. Nishiyama, T. Sakamoto, K. Yamaguchi, S. Hatakeyama, E. Shimizu, K. Katayama, Y. Yamada, S. Yamazaki, K. Iwasaki, C. Miyoshi, H. Funato, M. Yanagisawa, H. Ueno, S. Imoto, Y. Furukawa, N. Yoshida, K. Matsushima, H.R. Ueda, A. Miyajima, M. Nakanishi, Generation of a p16 reporter mouse and its use to characterize and target $p16^{high}$ cells in vivo, Cell Metabol. 32 (2020) 814–828, https://doi.org/10.1016/j.cmet.2020.09.006, e6.